Title

Monosodium Urate Crystal-Induced Pyroptotic Cell Death in Neutrophil and Macrophage Facilitates the Pathological Progress of Gout

Authors

Chen, Chen
Wang, Jingyun
Guo, Yiyang
et al.

Publication Date

2023-12-31

DOI

10.1002/smll.202308749

Peer reviewed

RESEARCH ARTICLE

NANO · MICRO small
www.small-journal.com

Monosodium Urate Crystal-Induced Pyroptotic Cell Death in Neutrophil and Macrophage Facilitates the Pathological Progress of Gout

Chen Chen, Jingyun Wang, Yiyang Guo, Min Li, Kaijun Yang, Yang Liu, Dan Ge, Yong Liu, Changying Xue, Tian Xia, and Bingbing Sun**

Monosodium urate (MSU) crystal deposition in joints can lead to the infiltration of neutrophils and macrophages, and their activation plays a critical role in the pathological progress of gout. However, the role of MSU crystal physicochemical properties in inducing cell death in neutrophil and macrophage is still unclear. In this study, MSU crystals of different sizes are synthesized to explore the role of pyroptosis in gout. It is demonstrated that MSU crystals induce size-dependent pyroptotic cell death in bone marrow-derived neutrophils (BMNs) and bone marrow-derived macrophages (BMDMs) by triggering NLRP3 inflammasome-dependent caspase-1 activation and subsequent formation of N-GSDMD. Furthermore, it is demonstrated that the size of MSU crystal also determines the formation of neutrophil extracellular traps (NETs) and aggregated neutrophil extracellular traps (aggNETs), which are promoted by the addition of interleukin-1β (IL-1β). Based on these mechanistic understandings, it is shown that N-GSDMD oligomerization inhibitor, dimethyl fumarate (DMF), inhibits MSU crystal-induced pyroptosis in BMNs and J774A.1 cells, and it further alleviates the acute inflammatory response in MSU crystals-induced gout mice model. This study elucidates that MSU crystal-induced pyroptosis in neutrophil and macrophage is critical for the pathological progress of gout, and provides a new therapeutic approach for the treatment of gout.

1. Introduction

Gout is an inflammatory disease induced by the precipitation and accumulation of monosodium urate (MSU) crystals, which exhibits an acute and self-limiting inflammatory response.[1–2] The supersaturation level of serum urate during compromised metabolic activity enables the crystallization of uric acid to form MSU crystals in the joint and surrounding tissues, which could promote the infiltration and activation of immune cells, e.g., neutrophils, macrophages, *etc.*, and further determine the pathological progress of gout.[3–6]

Pyroptosis is an inflammatory and lytic form of programmed cell death that is triggered by the inflammasomes activation and executed by pore-forming effector proteins.[7] It has been shown that pyroptosis plays a critical role in host immune defense against various invading pathogen infection.[8] However, excessive pyroptosis could induce continuous inflammatory responses, which are closely associated with

C. Chen, Y. Guo, M. Li, K. Yang, Y. Liu, D. Ge, B. Sun
State Key Laboratory of Fine Chemicals
Dalian University of Technology
2 Linggong Road, Dalian 116024, China
E-mail: bingbingsun@dlut.edu.cn

C. Chen, J. Wang, C. Xue
School of Bioengineering
Dalian University of Technology
2 Linggong Road, Dalian 116024, China

Y. Guo, M. Li, Y. Liu, D. Ge, B. Sun
School of Chemical Engineering
Dalian University of Technology
2 Linggong Road, Dalian 116024, China

Y. Guo, M. Li, Y. Liu, D. Ge, B. Sun
Frontiers Science Center for Smart Materials Oriented Chemical Engineering
School of Chemical Engineering
Dalian University of Technology
Dalian 116024, China

Y. Liu
Department of Hand Surgery
the Fifth Hospital of Harbin
Harbin 150040, China

T. Xia
Division of NanoMedicine
Department of Medicine
University of California
Los Angeles, CA 90095, USA
E-mail: txia@ucla.edu

The ORCID identification number(s) for the author(s) of this article can be found under https://doi.org/10.1002/smll.202308749

DOI: 10.1002/smll.202308749

the occurrence of acute and chronic inflammatory diseases, e.g., Alzheimer's disease, type 2 diabetes, gout, etc.[9–11] During a gout attack, the neutrophil and macrophage in the joints are activated by the deposition of MSU crystals to trigger an acute inflammatory response, which is crucial for the occurrence and resolution of gout.[6,12,13] It was demonstrated that the interaction between MSU crystals and neutrophils could induce the production of IL-1β by triggering the NLRP3 inflammasome activation, suggesting that the pathological progress of gout may be influenced by neutrophil-derived IL-1β.[14–16] Goldberg et al. demonstrated that the NLRP3 inflammasome activation in neutrophils has been indicated as a major source of IL-1β, which promoted the acute inflammatory response in a gout model in rats.[17] However, the important role of pyroptotic cell death of neutrophils induced by MSU crystals in gout has not been elucidated. Additionally, it has been demonstrated that MSU crystals could lead to the production of IL-1β by triggering the NLRP3 inflammasome activation in macrophage.[13,18] Hao et al. showed that MSU crystal-induced pyroptosis by activating bromodomain-containing protein 4 (BRD4)-related signaling pathway in macrophage, and BRD4-specific inhibitor could inhibit MSU crystals-induced pyroptosis in vitro and attenuate the acute inflammatory response in rats model of acute gout.[19] In our previous study, it was shown that the characteristics of MSU crystals mediated IL-1β production in a NLRP3 inflammasome-dependent manner in macrophages.[20] However, there is insufficient understanding of whether the characteristics of MSU crystals determine pyroptosis in macrophages during the occurrence of gout. Therefore, elucidating the role of physical properties of MSU crystals in pyroptotic cell death in neutrophil and macrophage would facilitate the understanding of the pathological progress of gout.

Herein, the effect of MSU crystal size on pyroptosis in neutrophil and macrophage was determined. MSU crystals were shown to induce size-dependent pyroptosis in neutrophil and macrophage by activating NLRP3 inflammasome and subsequent GSDMD cleavage. Furthermore, the formation of neutrophil extracellular traps (NETs) and aggregated neutrophil extracellular traps (aggNETs) were also dependent on the MSU crystal size in neutrophils, and the addition of IL-1β significantly promoted their formation. Based on these mechanistic understandings, dimethyl fumarate (DMF) was demonstrated to inhibit MSU crystals-induced pyroptosis in vitro and alleviate the inflammatory response on the joint site by targeting GSDMD in MSU crystals-induced gout. This study reveals the role of pyroptosis induced by MSU crystal in acute gout, and further provides a new therapy to alleviate the inflammatory response of gout.

2. Results

2.1. Preparation and Characterization of MSU Crystals

Monosodium urate (MSU) crystal was prepared according to our established method.[20] In a supersaturated uric acid solution, the nucleation process of MSU crystals could be controlled by sodium ion concentration. By tuning the nucleation and growth, MSU crystals with different sizes were synthesized. Scanning electron microscopy (SEM) and bright-field optical microscope analysis demonstrated that MSU crystals with uniform sizes were obtained (**Figure 1**A; Figure S1, Supporting Information). With the increase in sodium ion concentration, the length of MSU crystals became shorter.[20] Size distribution analysis showed that the primary lengths of MSU crystals were 23 ± 5 µm and 7 ± 2 µm for MSU-L and MSU-S, respectively (Figure 1B). X-ray diffraction (XRD) analysis showed that the crystal structures of synthesized MSU crystals were in agreement with the previously reported study (Figure 1C).[21]

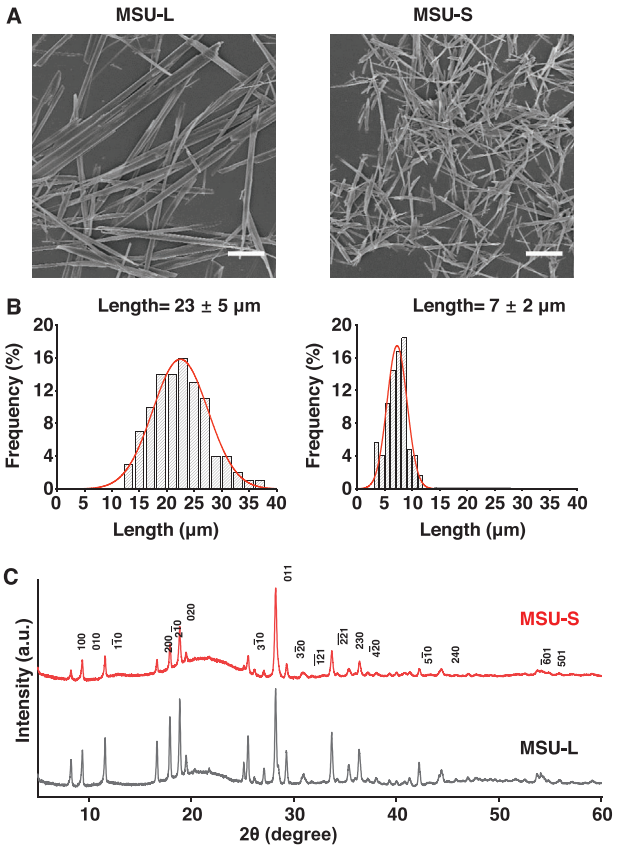

Figure 1. The characterization of MSU crystals. A) Representative SEM images and B) the length distribution analysis of MSU-L and MSU-S. SEM images of MSU crystals were used to measure the length by Image J software. At least 100 crystals were counted for the distribution analysis. Scale bar, 5 µm. C) XRD patterns of MSU-L and MSU-S.

2.2. MSU Crystals Induce Size-Dependent Pyroptosis in Neutrophil and Macrophage

During inflammation, neutrophils are among the first infiltrated cells in the inflamed region, which is critical for the progress of inflammatory diseases.[22–23] MSU crystal, a potent damage-associated molecular pattern (DAMP), has been demonstrated to be able to induce abundant neutrophil infiltration in acute peritonitis and gout in the previous study.[13,20] Thus, bone marrow-derived neutrophils (BMNs) were isolated to determine the MSU crystal-induced inflammatory response of gout. The flow cytometry analysis showed that the purity of primary neutrophils ($CD11b^+Ly6G^+$) was 94.9%. and the chromogenic Limulus amebocyte lysate assay demonstrated that there was no bacterial contamination in MSU crystals (Figures S2 and S3, Supporting

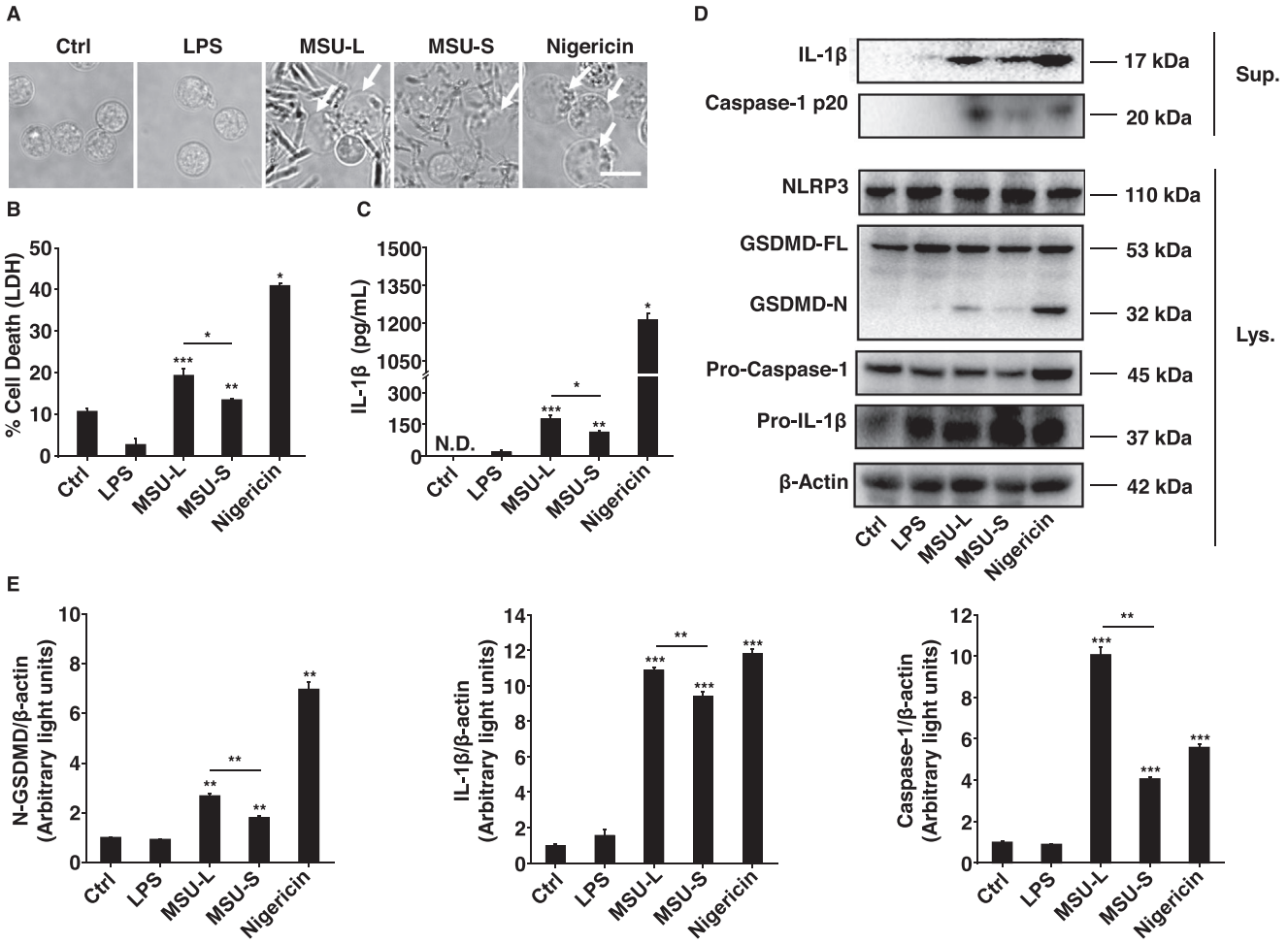

Figure 2. MSU crystals induced pyroptosis in primary mouse neutrophils. A) Representative images of morphological changes in neutrophils after exposure to MSU crystals (250 μg mL^{-1}, 12 h) or nigericin (10 μM, 12 h). Scale bar, 10 μm. B) The lactate dehydrogenase (LDH) release analysis. Lipopolysaccharide (LPS)-primed neutrophils (200 ng mL^{-1}, 4 h) were stimulated with MSU crystals (250 μg mL^{-1}) or Nigericin (10 μM) for 12 h. LDH release was determined by LDH cytotoxicity assay. Nigericin was a positive control. C) The IL-1β release analysis. LPS-primed neutrophils (200 ng mL^{-1}, 4 h) were exposed to MSU crystals (250 μg mL^{-1}) for 24 h. IL-1β release was determined by ELISA. D) LPS-primed neutrophils were treated with MSU crystals (250 μg mL^{-1}, 12 h), and the expressions of proteins in supernatants (Sup.) and cell extracts (Lys.) were analyzed by immunoblotting. E) The normalization form of N-GSDMD, IL-1β, and caspase-1 expression to β-actin. Data are presented as the means ± S.D. (n = 3). Statistical significance was determined by a two-tailed Student's t-test. $^{*}p < 0.05$, $^{**}p < 0.01$, $^{***}p < 0.001$.

Information). After exposure to MSU crystals, morphological changes in neutrophils were observed. It was demonstrated that MSU crystals led to significant cell swelling and membrane ballooning in BMNs (**Figure** 2A). This phenomenon was in accordance with the occurrence of pyroptosis.[24] It was shown that the MSU crystals induced LDH release in a size-dependent manner in BMNs, and MSU-L-induced LDH release was significantly more than that of MSU-S (Figure 2B). Furthermore, the production of interleukin-1β (IL-1β) was used to determine the pyroptotic cell death in BMNs. The ELISA analysis showed that MSU-L induced a higher level of IL-1β release in comparison to MSU-S in BMNs, suggesting the occurrence of pyroptosis in neutrophils (Figure 2C). A positive control, Nigericin, also induced pyroptosis in BMNs.

It has been demonstrated that NLRP3 inflammasome plays a crucial role in pyroptotic cell death in neutrophils.[25] Immunoblotting analysis showed a higher degree of NLRP3 and pro-IL-1β expression in LPS-priming neutrophil in comparison to the untreated group (Figure 2D). After the challenge by MSU crystals, it was shown that cleaved caspase-1 and IL-1β release were increased, which indicated that the activation of inflammatory caspase-1 was required for mature IL-1β production in BMNs (Figure 2D,E). NLRP3 inflammasome activation could drive cleavage of GSDMD into the activated N-GSDMD fragment.[26] Immunoblotting results further showed that MSU crystals led to the N-GSDMD formation in BMNs, and the MSU-L-treated cells induced higher expression of N-GSDMD, suggesting that MSU crystals could drive GSDMD-dependent neutrophil pyroptosis in a size-dependent manner (Figure 2D,E). Taken together, these results indicated that caspase-1-dependent GSDMD activation mediated the MSU crystal-induced pyroptosis in neutrophils.

Additionally, the role of MSU crystal size on pyroptosis in macrophages was determined in bone marrow-derived

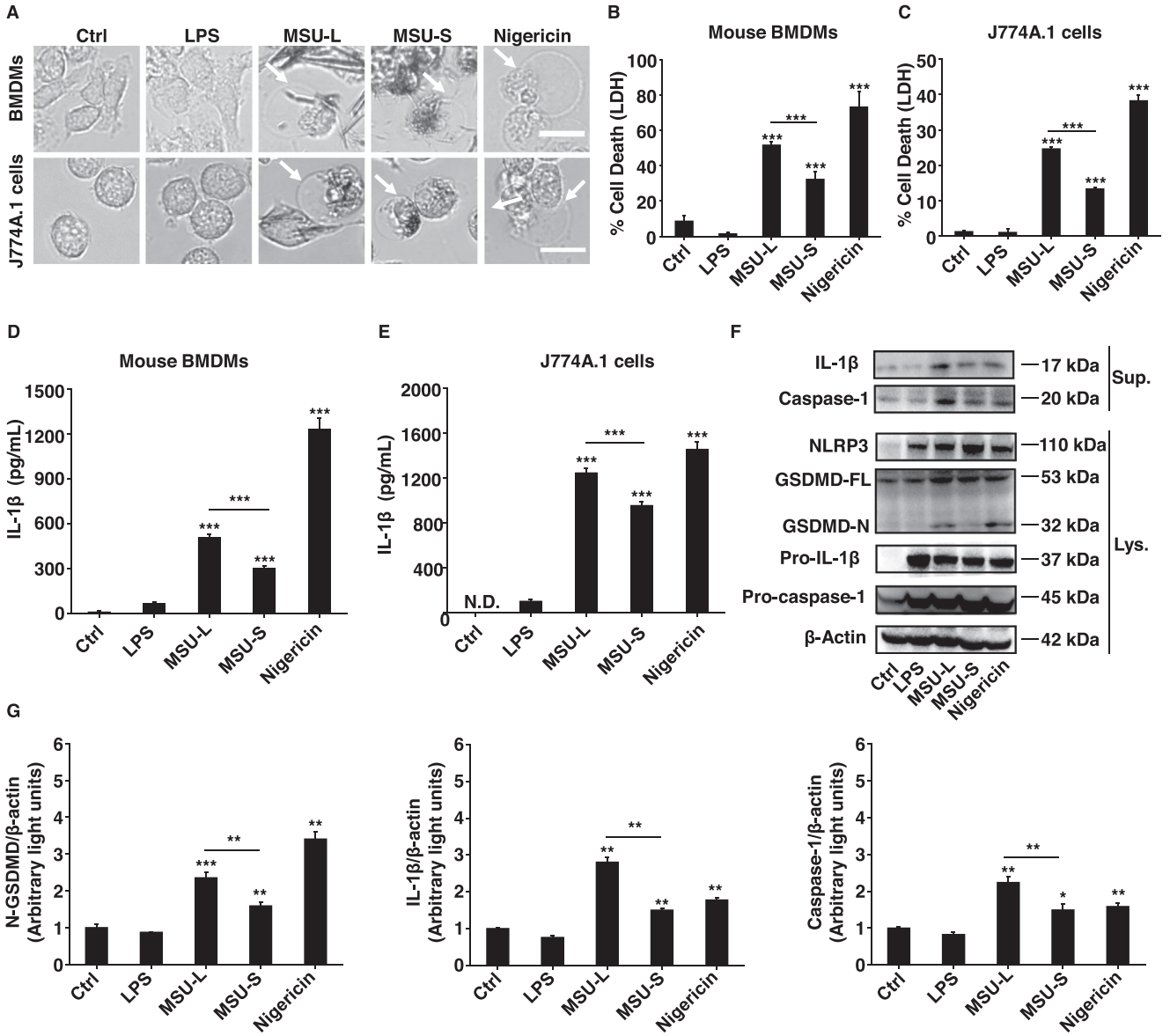

Figure 3. Induction of pyroptosis by MSU crystals in mouse macrophages. A) Representative morphologies of BMDMs and J774A.1 cells after exposure to MSU crystals. The white arrow indicates cell swelling and membrane blebbing. Scale bar, 20 μm. B,C) The lactate dehydrogenase (LDH) release analysis. D,E) The analysis of IL-1β production. Lipopolysaccharide (LPS)-primed (500 ng mL^{-1}) BMDMs and J774A.1 cells were stimulated with MSU crystals (200 μg mL^{-1}), and the release of LDH and IL-1β was determined by LDH cytotoxicity reagent and ELISA. Nigericin was a positive control. F) The expression of related proteins in supernatants (Sup.) and cell extracts (Lys.) after LPS-primed J774A.1 cells were exposed to MSU-L and MSU-S (200 μg mL^{-1}, 6 h) or Nigericin (10 μM, 2 h). G) The normalization form of N-GSDMD, IL-1β, and caspase-1 expression to β-actin. Data are presented as the means ± S.D. (n = 3). Statistical significance was determined by a two-tailed Student's t-test. $^{*}p < 0.05$, $^{**}p < 0.01$, $^{***}p < 0.001$.

macrophages (BMDMs) and J774A.1 cells. The cell swelling and cell membrane blebbing were observed after stimulation with MSU-L and MSU-S in macrophage, and the cell membrane permeability was increased in J774A.1 cells (**Figure 3**A; Figure S4, Supporting Information). Furthermore, MSU crystals induced significantly size-dependent LDH release and IL-1β production in macrophage (Figure 3B–E). Western blotting showed that the NLRP3 and pro-IL-1β expressions were increased after priming with LPS, and MSU crystals induced size-dependent activation of caspase-1 and N-GSDMD formation (Figure 3F,G). Moreover, the LDH release and IL-1β production induced by MSU crystals in NLRP3$^{-/-}$ BMDMs were inhibited (Figure S6, Supporting Information). Thus, these results demonstrated that the size of MSU crystals determined GSDMD-dependent pyroptosis in macrophages.

2.3. MSU Crystals Induce Size-Dependent NET and aggNET Formation

It has been demonstrated that activated neutrophils not only induce the production of cytokines but also lead to NETs

formation, which further promote the progress of inflammatory diseases including gout.[6,27,28] NETs are web-like structures, which are composed of a mixture of chromatin decorated with histones and neutrophil granules, e.g., elastase and myeloperoxidase.[29] To determine the effect of MSU crystal size on the NET formation, neutrophils were exposed to MSU-L and MSU-S, and PMA was a positive control. The immunofluorescence assay was used to determine NET

formation by staining neutrophil elastase (NE) and DNA. It was demonstrated that MSU-L induced more significant NET formation than MSU-S in BMNs (**Figure** 4A). Furthermore, the extracellular DNA content was quantitatively determined by fluorometric measurement method to assess the formation of NET. It was shown that MSU crystals led to the release of extracellular DNA in a size-dependent manner (Figure 4B). These results indicated that the physical properties of MSU crystals play a critical role in NET formation. IL-1β has been identified as a key cytokine in the progress of gout, thus its role in the formation of NET was determined.[30] The immunofluorescence assay indicated that the addition of recombinant IL-1β significantly promoted NET formation triggered by MSU crystals (Figure 4C). To further assess the role of IL-1β in NET formation, an anti-IL-1β neutralizing antibody was used to suppress IL-1β activity. It was demonstrated that the formation of NET triggered by MSU crystals was inhibited by neutralizing antibodies, and its inhibiting effect was in a concentration-dependent manner (Figure 4C). Anti-IL-1β neutralizing antibody alone did not affect MSU crystal-induced NET formation (Figure 4C). Furthermore, MSU crystals could stimulate neutrophils to form aggregated NET (aggNETs), which was the structural foundation of gout tophi.[6] Optical microscopy images showed that neutrophils exposed to MSU-L induced more significant aggNET formation compared to MSU-S, and the formation of aggNET was enhanced following the recombinant IL-1β treatment (Figure S5, Supporting Information). Altogether, those results suggested that MSU crystals led to size-dependent NET and aggNET formation, which were promoted *via* the addition of IL-1β.

2.4. DMF Treatment Alleviates the Acute Inflammatory Response in Neutrophil and Macrophage

MSU crystal-induced GSDMD-dependent pyroptosis in neutrophil, and dimethyl fumarate (DMF) have been shown to induce GSDMD succination by reacting with critical cysteine residues to inhibit pyroptosis.[31] Thus, DMF was selected as a therapeutic agent to alleviate the inflammatory response in acute gout by suppressing MSU crystal-induced pyroptosis. DMF did not exhibit cytotoxicity at concentrations of 25 and 50 μM in vitro (Figure S7, Supporting Information). The ELISA and western blotting analysis showed that DMF suppressed the production of IL-1β in BMNs (**Figure** 5A,C). Meanwhile, the production of TNF-α stimulated by MSU crystals in BMNs was inhibited after DMF treatment (Figure 5B). Furthermore, western blotting indicated that DMF did not suppress the expression of pro-caspase-1 and pro-IL-1β, however, it dramatically inhibited the formation of N-GSDMD and caspase-1 activation,

confirming the effect of DMF in inhibiting pyroptosis (Figure 5C, D). Therefore, these results demonstrated that DMF treatment could alleviate MSU crystals-induced acute inflammatory response by inhibiting pyroptosis in BMNs. Additionally, it was shown that DMF treatment could inhibit the formation of N-GSDMD, and increase plasma membrane permeability and IL-1β production triggered by MSU crystals in macrophage (Figure S8, Supporting Information).

2.5. DMF Treatment Mitigates the Acute Inflammatory Response in MSU Crystals-induced Gout

Based on the above findings that MSU crystals promoted the occurrence of pyroptosis and DMF could inhibit MSU crystal-induced the release of cytokine in vitro, the anti-inflammatory effects of DMF were further determined in vivo. To reduce side effects and prolong the retention of DMF in vivo, poly (lactic-co-glycolic acid) (PLGA) nanoparticles were used to encapsulate DMF, which were named PLGA-DMF.[32] Transmission electron microscope (TEM) analysis showed that PLGA nanoparticles (PLGA) and PLGA-DMF with uniform sizes and morphologies were prepared (**Figure** 6A). It was demonstrated that the hydrodynamic sizes of PLGA-NPs and PLGA-DMF in water were 235.1 ± 4.9 and 239.8 ± 4.9 nm, respectively (Figure 6B). Zeta potential measurement demonstrated that PLGA-NPs and PLGA-DMF carried negative charges, and they were −30 and −35 mV, respectively (Figure 6C). DMF could be slowly released from DMF-PLGA (Figure S9, Supporting Information). DMF and PLGA-DMF were administered by intraperitoneal and in situ injection, respectively. The longer MSU crystals were injected into the mouse knee

joints to establish a mouse model of gout, which were indicated by joint swelling and H&E staining (**Figure** 7A; Figure S10, Supporting Information). It was shown that MSU crystal-induced acute joint swelling was mitigated after DMF and PLGA-DMF treatment (Figure S10, Supporting Information). H&E staining showed that cell infiltration induced by MSU crystals (black arrow pointed)

was alleviated by DMF and PLGA-DMF treatment, and the degree of joint inflammation was significantly inhibited following their treatment (Figure 7A,B). Furthermore, myeloperoxidase (MPO), a representative marker of neutrophil infiltration, was used to further determine the neutrophil infiltration. It was demonstrated that both DMF and PLGA-DMF treatment suppressed MPO activity in arthritis regions induced by MSU crystals, further indicating that DMF and PLGA-DMF treatment could reduce the neutrophil infiltration into the knee joints of MSU crystal-treated mice (Figure 7C). Moreover, ELISA analysis showed that the deposition of MSU crystals induced significant secretion of IL-1β, IL-6, and TNF-α, while DMF and PLGA-DMF treatment reduced their level in the knee region (Figure 7D–F). To further determine the long-term inhibitory role of PLGA-DMF in the inflammatory response of gout, the cytokine production in the knee region after PLGA-DMF treatment for 72 h was determined. It was demonstrated that IL-1β, IL-6, and TNF-α production was inhibited by PLGA-DMF treatment, however, free DMF treatment did not reduce the release of these cytokines (Figure 7G,H; Figure S11, Supporting Information). This result indicated that PLGA-DMF treatment could prolong the therapy effect on acute inflammation induced by MSU crystals in vivo.

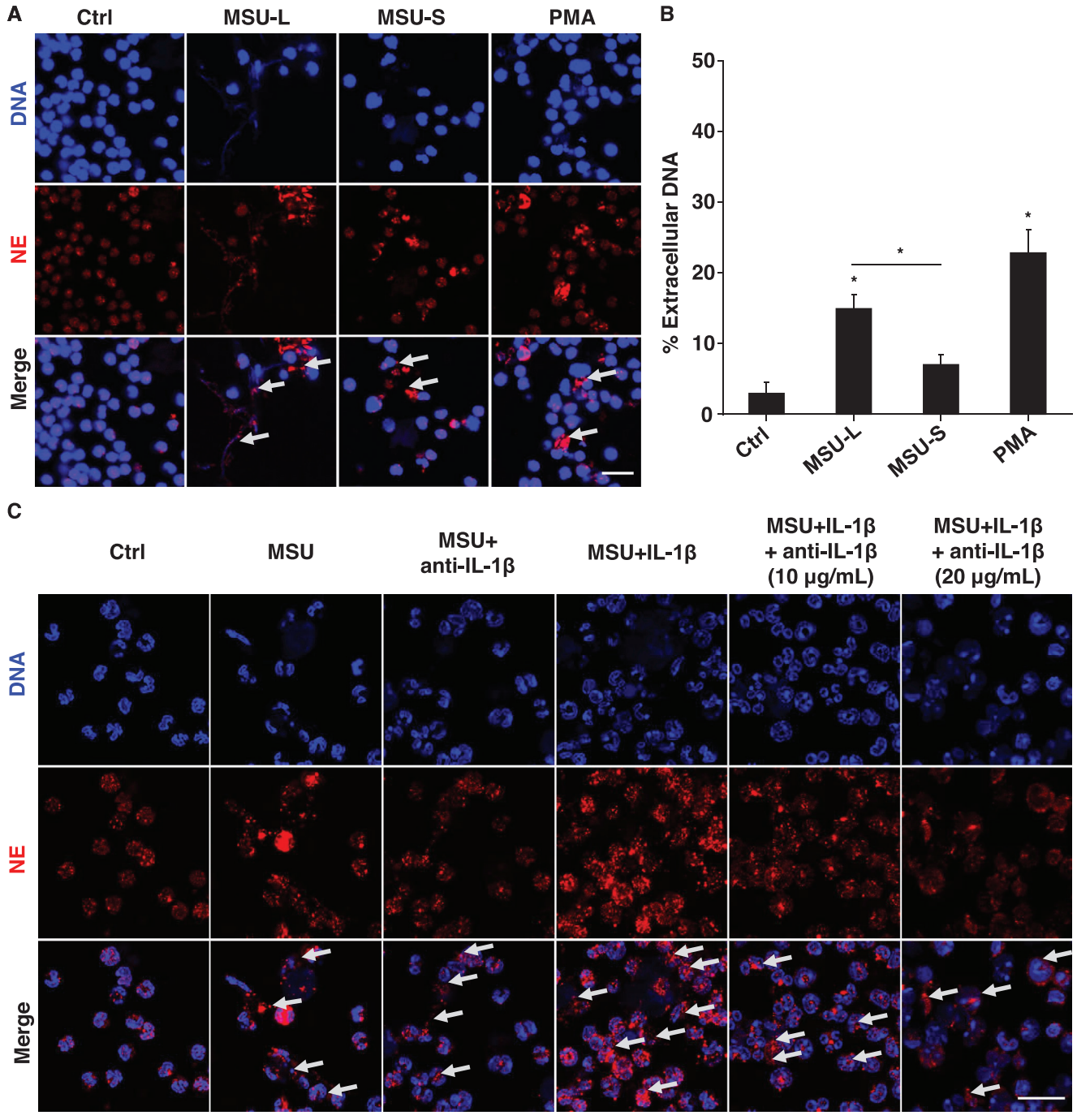

Figure 4. MSU crystals promoted NET formation in vitro. A) Representative images of NET formation. Neutrophils were exposed to MSU crystals (250 μg mL^{-1}) for 6 h, and neutrophil elastase (NE) and Hoechst 33342 were used to determine NET formation by immunofluorescence. The PMA was used as a positive control (200 nM, 6 h). B) Quantification of NET formation. SYTOX Green was used to stain the extracellular DNA. The PMA was used as a positive control (200 nM, 3 h). C) The effect of IL-1β on NET formation. Neutrophils were stimulated with MSU crystals (250 μg mL^{-1}) by the addition of IL-1β (50 ng mL^{-1}) or neutralizing IL-1β antibody (10 or 20 μg mL^{-1}). To visualize NET formation, neutrophil elastase (NE) and DNA in neutrophils were stained with anti-NE antibody (red) and Hoechst 33342 (blue), respectively. The scale bar is 20 μm. Data are presented as the means ± S.D. (n = 3). Statistical significance was determined by a two-tailed Student's t-test. $^{*}p < 0.05$.

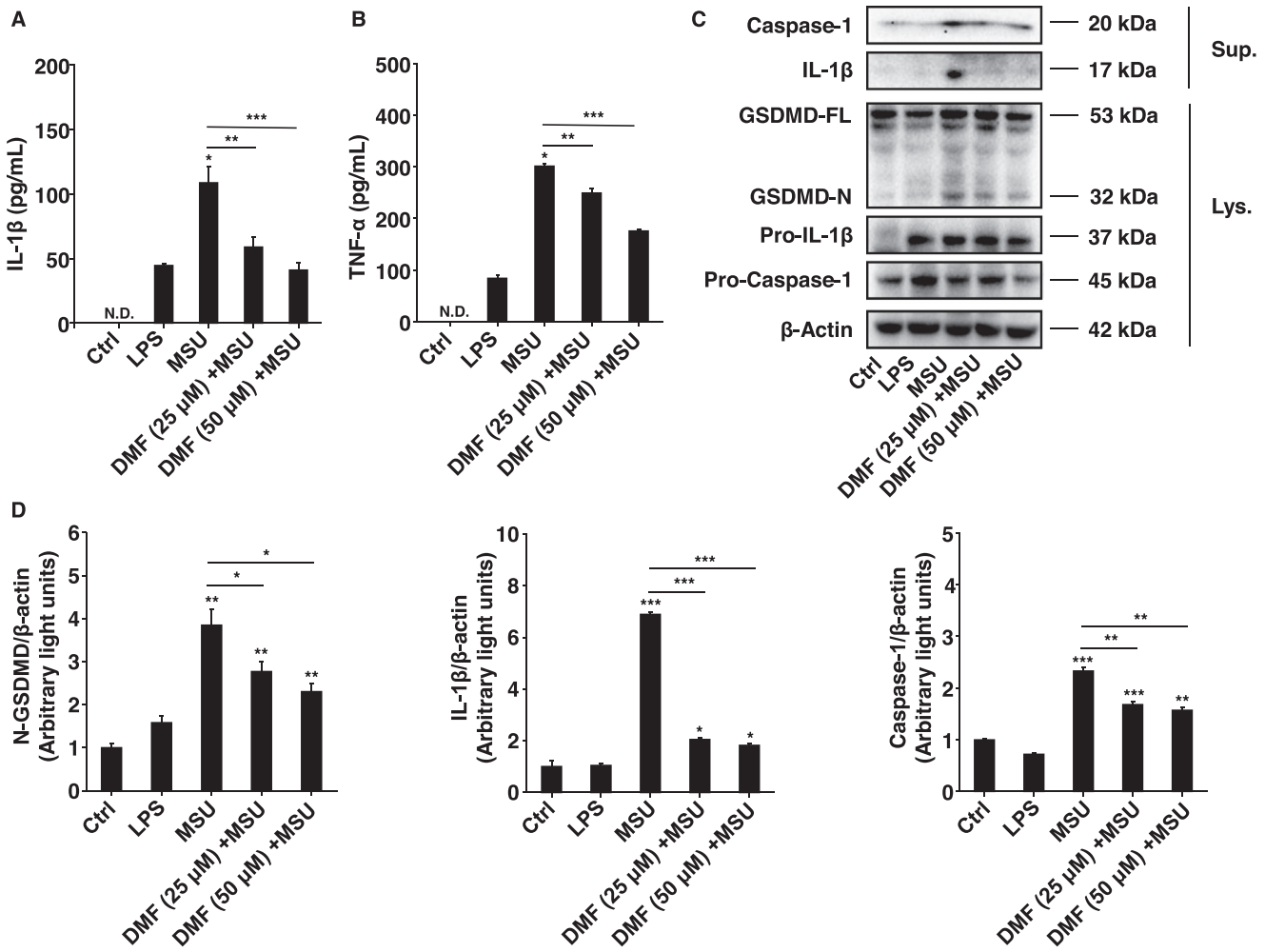

Figure 5. Dimethyl fumarate inhibited MSU crystal-induced pyroptosis in BMNs. A,B) The IL-1β and TNF-α release triggered by MSU crystals in BMNs. LPS-primed (200 ng mL^{-1}, 4 h) neutrophils were pre-treated with dimethyl fumarate for 1 h by the indicated concentration, then the cells were exposed to MSU crystals (200 μg mL^{-1}, 24 h). C) The level of protein in supernatants (Sup.) and cell extracts (Lys.) were determined by immunoblotting. D) The normalization form of N-GSDMD, IL-1β, and caspase-1 protein expression to β-actin. Data are presented as the means ± S.D. (n = 3). Statistical significance was determined by a two-tailed Student's t-test. $^{*}p < 0.05$, $^{**}p < 0.01$, $^{***}p < 0.001$.

Therefore, these results suggested that DMF and PLGA-DMF could mitigate the symptoms of MSU crystal-induced gout by suppressing pyroptosis to reduce cytokine production and immune cell infiltration, suggesting that DMF could be a potential candidate for gout treatment.

In order to further determine the effect of macrophage in acute gout, clodronate liposomes were used for macrophage depletion. MSU crystals were injected into the joint cavity to establish a mouse model of acute gout. The ELISA and H&E staining results showed that IL-1β production and leukocyte infiltration were significantly inhibited after macrophage depletion (Figure 7I,J). Furthermore, western blot analysis further showed that GSDMD cleavage and N-GSDMD formation induced by MSU crystals were suppressed in the clodronate liposome-treated group, suggesting the important role of pyroptosis in macrophage in the occurrence of acute gout (Figure 7K). However, MSU crystals could still induce IL-1β production, leukocyte infiltration, and GSDMD cleavage despite macrophage clearance, indicating the effect of pyroptotic cell death of neutrophils on the acute gout (Figure 7I,K).

3. Discussion

In this study, MSU crystals with different sizes were prepared to study the role of pyroptosis in neutrophils and macrophages for the pathogenesis of gout. It was shown that MSU crystals triggered GSDMD-dependent pyroptotic cell death in neutrophils and macrophages in a size-dependent manner. Furthermore, MSU crystals induced size-dependent NET and aggNET formation in neutrophils, and their formation was promoted in the presence of IL-1β. Additionally, DMF ameliorated MSU crystal-induced acute inflammatory response by suppressing GSDMD-dependent pyroptosis in vitro and in the MSU crystal-induced gout model.

MSU crystal-triggered inflammatory response in the acute gout phase is caused by activating innate immune response.[30]

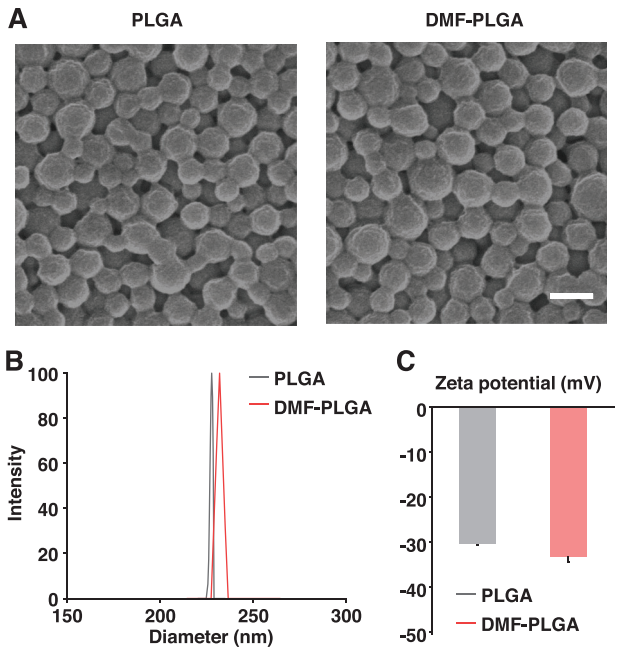

Figure 6. The synthesis and characterization of PLGA and PLGA-DMF nanoparticles. A) SEM images, B) size, and C) zeta potential. The scale bar is 200 nm.

Admittedly, the aspect ratio of MSU crystals in vivo is neither homogeneous nor static. It was influenced by several factors, e.g., temperature, pH, protein, and local ionic strength, etc. In our previous study, it was shown that the shape and aspect ratio of MSU crystals could determine the pathogenesis of gout in a gouty model in mice.[20] In the pathological process of gout, neutrophils and macrophages could infiltrate the inflammatory sites and be activated to promote the development of the disease.[33,34] NLRP3 inflammasome-mediated programmed cell death was demonstrated to be critical for the occurrence and development of inflammatory diseases.[10] It was shown that MSU crystals could induce pyroptosis in macrophages, which was determined by LDH release, GSDMD cleavage, and IL-1β production.[18,35] However, the role of pyroptosis in neutrophil have not been fully elucidated in gout.[15,17] In this study, it was indicated that MSU crystals induced the morphological changes and IL-1β and LDH release in a size-dependent manner in neutrophil, suggesting the occurrence of neutrophil pyroptosis (Figure 2A–C). Further mechanistic studies demonstrated that MSU crystal-triggered pyroptosis in neutrophils was driven by caspase-1 and subsequent GSDMD activation (Figure 2D). After macrophage depletion by injecting clodronate liposomes in a mouse gout arthritic model, IL-1β production and GSDMD cleavage in the joint were inhibited, however, they still occurred, partially suggesting the role of pyroptosis in neutrophil for pathological progress in MSU crystals-induced gout (Figure 7G–I). The pyroptotic cell death of neutrophils may explain the phenomenon of continuous occurrence in the inflammatory response during the acute phase of gout.[27] Moreover, it was shown that longer MSU crystals were more toxic than shorter ones in inducing the pyroptotic cell death of neutrophils and macrophages. The crucial role of the size of nanomaterials in pro-inflammatory response in macrophage have also been demonstrated in previously reported studies. Poland et al. showed that multiwalled nanotubes$_{long1\text{-}2}$ could induce a more significant inflammatory response than the nanotubes$_{tang1\text{-}2}$ in mouse model, and they were more like to trigger the frustrated phagocytosis and the generation of cytokines in macrophages.[36] Ma et al. demonstrated that larger graphene oxides exhibit stronger potential in promoting pro-inflammatory response than the smaller ones, which was dependent on their adsorption onto the cell membrane but not phagocytosis.[37] Therefore, these studies demonstrated that different types of macro- or nano-material could have significant differences in interaction mechanisms with macrophages, which determined their pro-inflammatory potencials.

It has been demonstrated that the morphology of MSU crystals derived from synovial fluid were predominantly needle-shaped particles in gouty patients.[21,38–40] Moreover, it was shown that the length of MSU crystals in synovial fluid was in the range of 1–20 µm.[1] A recent clinical study showed that the median length of MSU crystals from 20 joints in 17 patients was 21.2 µm.[41] Thus, the size range of our in-house synthesized MSU crystals shows clinical relevance. The physicochemical property-dependent oxidative stresses induced by nano-materials and crystal-materials have been demonstrated in reported studies. Li et al. reported that graphene oxide of large lateral size exhibited a stronger effect on pyroptosis than ones of large lateral size in Kupffer cells by triggering NADPH oxidase activation, calcium flux, mitochondrial ROS generation.[42] Du et al. showed that Stöber silica nanoparticles induced size-dependent pyroptosis in N9 cells, which was mediated by mitochondrial ROS generation and GSDMD cleavage.[43] Li et al. demonstrated that nano-silica induced more severe pyroptosis than micro-silica by elevating the ROS production in macrophages, which was involved in the silica-induced pulmonary inflammation.[44]

NET is an extracellular net-like structure, consisting of nuclear DNA and proteins released by activated neutrophils, which is involved in a variety of diseases, e.g., rheumatoid arthritis, systemic lupus erythematosus, and gout, etc. In this study, it was demonstrated that MSU crystals could induce pyroptosis by caspase-1-dependent GSDMD activation in neutrophils (Figure 2). In comparison, MSU crystal-induced NET formation may be mediated by NADPH oxidase-mediated ROS production, suggesting that oxidative stress is involved in MSU crystal-induced neutrophil activation.[6,45] In addition, multiple signaling pathway involved in MSU crystal-induced NET formation have been demonstrated in reported studies. Desai *et al.* showed that MSU crystal-induced NET formation was mediated by RIPK1-RIPK3-MLKL signaling.[46] Mitroulis *et al.* showed that IL-1β and autophagy-related signaling were in part involved in the MSU crystals-induced NET formation.[47] In our study, MSU crystals also induced the formation of NET and aggNET in neutrophils, and their formation were promoted by recombinant IL-1β (Figure 4). A potential mechanism of IL-1β to promote MSU crystals-induced NET formation is the interaction between IL-1β and IL-1β receptor. Mitroulis et al. demonstrated that synovial fluid from patients with active arthritis induced the formation of NET in healthy neutrophils, and its formation could be partially inhibited by both anti-IL-1β antibody and anakinra treatment, suggesting that the NET formation was related to IL-1 signaling.[47] Meher et al. showed that IL-1β treatment could induce NETosis

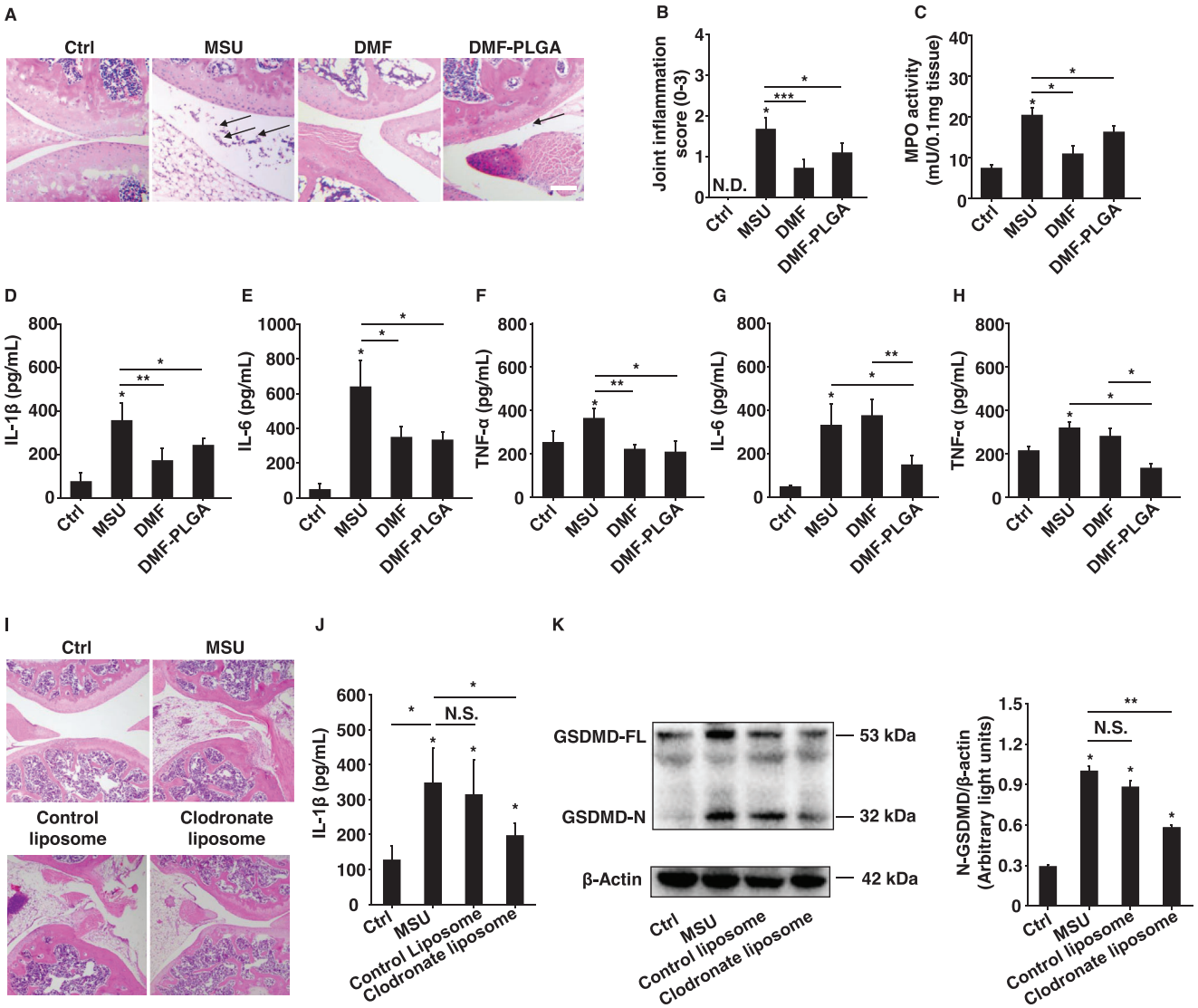

Figure 7. PLGA-DMF ameliorated the MSU crystals-induced acute gout and neutrophils mediated the occurrence of acute inflammatory response of arthritis. For the DMF treatment, DMF (50 mg kg^{-1}) was *i.a.* administered 2 h before MSU crystal injection (200 μg). For the PLGA-DMF treatment, PLGA-DMF (10 mg kg^{-1}) was injected into the joint cavity (n = 6). A) H&E staining images. Black arrow indicated infiltrated leucocytes. Scale bar, 100 μm. B,C) Joint score and MPO activity were analyzed after treatment for 24 h. D,F) IL-1β, IL-6, and TNF-α productions were analyzed by ELISA. G,H) IL-6 and TNF-α productions were determined after treatment for 72 h. For macrophage depletion, clodronate liposomes and control liposomes (200 μL) were intravenously injected via the tail vein. After 24 h, MSU crystals (200 μg) were injected into the knee joint. I) H&E staining images were used to determine the leucocyte infiltration (black arrow). Scale bar, 500 μm. J) The production of IL-1β. K) The cleavage of GSDMD. Data are presented as the means ± S.D. (n = 6). Statistical significance was determined by a two-tailed Student's t-test. $^{*}p < 0.05$, $^{**}p < 0.01$, $^{***}p < 0.001$, N.S.: no significance.

by the interaction between IL-1β and IL-1β receptor to trigger ceramide synthesis in human neutrophils, which play a crucial role in abdominal aortic aneurysm formation.[48] Another potential mechanism for the role of IL-1β in NET formation is effect of IL-1β on NADPH oxidase activation.[49] It was demonstrated that the NET formation induced by MSU crystals was dependent on NADPH oxidase, and the phosphorylation of the oxidase subunits could be enhanced by IL-1β, suggesting the interaction between IL-1β and NADPH oxidase plays a crucial role in NET formation.[6,50,51] Moreover, the role of pyroptosis in macrophage on NET formation has been demonstrated in many studies. Chen *et al.* demonstrated that NETs-derived high-mobility group box 1 (HMGB1) could induce cathepsin B release and caspase-1 activation by the receptor for advanced glycation end products (RAGE)-dynamin signaling pathway. It mediated the pyroptosis in macrophage in a cecal ligation and puncture (CLP) sepsis model in mice.[52] Cui *et al.* reported that LPS-induced NETs led to pyroptosis in the alveolar macrophage by priming the generation of ROS and subsequent activation of NLRP3 deubiquitination in CLP model.[53] Li *et al.* showed that the NETs led to pyroptosis in the alveolar macrophage in LPS-induced acute lung injury mouse model, which was dependent on the activation of the AIM2-ASC-caspase-1 signaling pathway.[54] Additionally, Liu *et al.* demonstrated that the pretreatment of alpha-linolenic acid

could mitigate the sepsis-driven acute lung injury (ALI)/acute respiratory distress syndrome (ARDS) by suppressing the NET-induced macrophage pyroptosis, which was dependent on the inhibition of pyrin inflammasome activation.[55] Therefore, inhibiting NET-driven pyroptosis in macrophage could be a new therapeutic strategy for the inflammatory diseases.

The occurrence of gout arthritis is due to the acute inflammation induced by MSU crystals in joints, subsequently driving a cascade response of other pro-inflammatory cytokines and chemokines.[27] Thus, the aim of gout treatment is to inhibit the acute inflammatory response. Currently, colchicine, nonsteroidal antiinflammatory drugs (NSAIDs), or corticosteroids are considered first-line drugs for gout treatment, and IL-1 inhibitors have also been used for the therapy of gout.[30] However, these drugs could induce an increased frequency of side effects, and novel anti-inflammatory therapies are also being studied. Pyroptosis, as an inflammatory cell death manner, has a crucial role in the pathogenesis of inflammatory diseases, and the inhibition of GSDMD cleavage has been proven to alleviate the symptoms of inflammatory diseases.[31,56] Ye et al. reported that GSDMD siRNA-Loaded PEI-Chol Lipopolymers could relieve MSU crystal-induced acute inflammation by inhibiting pyroptosis in acute gout.[57] Furthermore, it was shown that dimethyl fumarate could induce GSDMD succination by reacting with its critical cysteine residues to suppress GSDMD cleavage.[31,58] In this study, we showed that dimethyl fumarate (DMF) inhibited IL-1β production and the cleavage of GSDMD in vitro, and it alleviated the inflammatory cells infiltration and cytokines production in MSU crystal-induced gout by inhibiting pyroptosis (Figures 5 and 7). Consistent with these observations, recent studies demonstrated that GSDMD-dependent pyroptosis is crucial for the pathogenesis of MS, and inhibition of GSDMD activation by DMF provided a new strategy for multiple sclerosis therapy.[31,59] Another study by Kang et al. also showed that DMF dramatically ameliorate silicosis pathology by inhibiting pyroptosis, implicating a new drug for silicosis treatment.[60] Therefore, our study suggests that DMF could be used for gouty therapy by suppressing pyroptosis.

4. Conclusion

In this paper, MSU crystals induced physicochemical properties-dependent pyroptosis in neutrophils and macrophages by activating the NLRP3 inflammasome to trigger the formation of N-GSDMD. MSU crystals also led to NET and aggNET formation in a size-dependent manner. Moreover, DMF was demonstrated to inhibit pyroptosis by suppressing the formation of N-GSDMD in BMNs and J774A.1 cells, and it alleviated the MSU crystals-induced inflammatory responses by inhibiting pyroptosis in gout. The results highlight the role of pyroptosis in neutrophil and macrophage during the pathological progress of gout attack and provide a potential therapy for gout.

Supporting Information

Supporting Information is available from the Wiley Online Library or from the author.

Acknowledgements

This work was supported by the National Natural Science Foundation of China (U22A20455), National Key Research and Development Program of China (2022YFC2304305), and Fundamental Research Funds for the Central Universities (DUT21ZD216, DUT22LAB601, and DUT22YG120). All animal experiments were in accordance with the guidelines approved by the Institutional Animal Care and Use Committee of Dalian University of Technology (Approval number: 2018–028). Chen Chen and Jingyun Wang contributed equally to this work.

Conflict of Interest

The authors declare no conflict of interest.

Data Availability Statement

The data that support the findings of this study are available from the corresponding author upon reasonable request.

Keywords

Dimethyl fumarate, Gout, Macrophage, Monosodium urate crystals, Neutrophil, Neutrophil extracellular traps, Pyroptosis

Received: September 30, 2023
Revised: December 9, 2023
Published online:

[1] N. Dalbeth, A. L. Gosling, A. Gaffo, A. Abhishek, *Lancet* **2021**, *397*, 1843.
[2] M. Dehlin, L. Jacobsson, E. Roddy, *Nat. Rev. Rheumatol.* **2020**, *16*, 380.
[3] A. K. So, F. Martinon, *Nat. Rev. Rheumatol.* **2017**, *13*, 639.
[4] N. Dalbeth, H. K. Choi, L. A. B. Joosten, P. P. Khanna, H. Matsuo, F. Perez-Ruiz, L. K. Stamp, *Nat. Rev. Dis. Primers* **2019**, *5*, 69.
[5] C. Yin, B. Liu, Y. Li, X. Li, J. Wang, R. Chen, Y. Tai, Q. Shou, P. Wang, X. Shao, Y.i Liang, H. Zhou, W. Mi, J. Fang, B. Liu, *Theranostics* **2020**, *10*, 12189.
[6] C. Schauer, C. Janko, L. E. Munoz, Y.i Zhao, D. Kienhöfer, B. Frey, M. Lell, B. Manger, J. Rech, E. Naschberger, R. Holmdahl, V. Krenn, T. Harrer, I. Jeremic, R. Bilyy, G. Schett, M. Hoffmann, M. Herrmann, *Nat. Med.* **2014**, *20*, 511.
[7] Q. Wang, J. Wu, Y. Zeng, K. Chen, C. Wang, S. Yang, N. Sun, H. Chen, K. Duan, G. Zeng, *Clin. Chim. Acta* **2020**, *510*, 62.
[8] Y.u Guo, L. Li, T. Xu, X. Guo, C. Wang, Y. Li, Y. Yang, D. Yang, B. Sun, X. Zhao, G. Shao, X. Qi, *J. Clin. Invest.* **2020**, *130*, 6301.
[9] W. Gao, X. Wang, Y. Zhou, X. Wang, Y. Yu, *Signal Transduct Target Ther* **2022**, *7*, 196.
[10] P. Yu, X.u Zhang, N. Liu, L. Tang, C. Peng, X. Chen, *Signal Transduct Target Ther* **2021**, *6*, 128.
[11] L. Qiao, Y. Shen, S. Zhang, M. Wang, G. Lv, Q. Dou, C. Li, *BMEMat* **2023**, *1*, 12011.
[12] Y. Lin, T. Luo, A. Weng, X. Huang, Y. Yao, Z. Fu, Y. Li, A. Liu, X. Li, D. Chen, H. Pan, *Front Immunol* **2020**, 11.
[13] F. Martinon, V. Pétrilli, A. Mayor, A. Tardivel, J. Tschopp, *Nature* **2006**, *440*, 237.
[14] C. J. Roberge, J. Grassi, R. Médicis, Y. Frobert, A. Lussier, P. H. Naccache, P. E. Poubelle, *Agents Actions Suppl* **1991**, *34*, 38.
[15] A. K. Mankan, T. Dau, D. Jenne, V. Hornung, *Eur. J. Immunol.* **2012**, *42*, 710.

[16] L.-S. Rousseau, G. Paré, A. Lachhab, P. H. Naccache, F. Marceau, P. Tessier, M. Pelletier, M. Fernandes, *J Leukoc Biol* **2017**, *102*, 805.
[17] E. L. Goldberg, J. L. Asher, R. D. Molony, A. C. Shaw, C. J. Zeiss, C. Wang, L. A. Morozova-Roche, R. I. Herzog, A. Iwasaki, V. D. Dixit, *Cell Rep.* **2017**, *18*, 2077.
[18] H. Li, W. Jiang, S. Ye, M. Zhou, C. Liu, X. Yang, K. Hao, Q. Hu, *Cell Death Dis.* **2020**, *11*, 394.
[19] K. Hao, W. Jiang, M. Zhou, H. Li, Y. Chen, F. Jiang, Q. Hu, *Int J Biol Sci* **2020**, *16*, 3163.
[20] C. Chen, J. Wang, Z. Liang, M. Li, D. Fu, L. Zhang, X. Yang, Y. Guo, D. Ge, Y. Liu, B. Sun, *Biomater Adv* **2022**, *139*, 213005.
[21] R. G. E. Molloy, W. Sun, J. Chen, W. Zhou, *Chem. Commun. (Camb)* **2019**, *55*, 2178.
[22] V. Papayannopoulos, *Nat. Rev. Immunol.* **2018**, *18*, 134.
[23] V. Poli, I. Zanoni, *Trends Microbiol.* **2023**, *31*, 280.
[24] V. Mirshafiee, B. Sun, C. H. Chang, Y.u-P. Liao, W. Jiang, J. Jiang, X. Liu, X. Wang, T. Xia, A. E. Nel, *ACS Nano* **2018**, *12*, 3836.
[25] D. Chauhan, D. Demon, L. Vande Walle, O. Paerewijck, A. Zecchin, L. Bosseler, K. Santoni, R. Planès, S. Ribo, A. Fossoul, A. Gonçalves, H. Van Gorp, N. Van Opdenbosch, F. Van Hauwermeiren, E. Meunier, A. Wullaert, M. Lamkanfi, *EMBO Rep.* **2022**, *23*, 54277.
[26] K. Santoni, D. Pericat, L. Gorse, J. Buyck, M. Pinilla, L. Prouvensier, S. Bagayoko, A. Hessel, S. A. Leon-Icaza, E. Bellard, S. Mazères, E. Doz-Deblauwe, N. Winter, C. Paget, J.-P. Girard, C. T. N. Pham, C. Cougoule, R. Poincloux, M. Lamkanfi, E. Lefrançais, E. Meunier, R. Planès, *PLoS Pathog.* **2022**, *18*, 1010305.
[27] J. Desai, S. Steiger, H.-J. Anders, *Trends Mol. Med.* **2017**, *23*, 756.
[28] K. W. Chen, M. Monteleone, D. Boucher, G. Sollberger, D. Ramnath, N. D. Condon, J. B. von Pein, P. Broz, M. J. Sweet, K. Schroder, *Sci. Immunol.* **2018**, *3*, eaar6676.
[29] G. Wigerblad, M. J. Kaplan, *Nat. Rev. Immunol.* **2023**, *23*, 274.
[30] J. Zhao, K. Wei, P. Jiang, C. Chang, L. Xu, L. Xu, Y. Shi, S. Guo, Y.u Xue, D. He, *Front Immunol* **2022**, *13*, 888306.
[31] F. Humphries, L. Shmuel-Galia, N. Ketelut-Carneiro, S. Li, B. Wang, V. V. Nemmara, R. Wilson, Z. Jiang, F. Khalighinejad, K. Muneeruddin, S. A. Shaffer, R. Dutta, C. Ionete, S. Pesiridis, S. Yang, P. R. Thompson, K. A. Fitzgerald, *Science* **2020**, *369*, 1633.
[32] Z. Belhadj, Y. Qie, R. P. Carney, Y. Li, G. Nie, *BMEMat* **2023**, *1*, 12018.
[33] C. Jin, P. Frayssinet, R. Pelker, D. Cwirka, B.o Hu, A. Vignery, S. C. Eisenbarth, R. A. Flavell, *Proc. Natl. Acad. Sci. USA* **2011**, *108*, 14867.
[34] P. Duewell, H. Kono, K. J. Rayner, C. M. Sirois, G. Vladimer, F. G. Bauernfeind, G. S. Abela, L. Franchi, G. Nuñez, M. Schnurr, T. Espevik, E. Lien, K. A. Fitzgerald, K. L. Rock, K. J. Moore, S. D. Wright, V. Hornung, E. Latz, *Nature* **2010**, *464*, 1357.
[35] F. Renaudin, L. Orliaguet, F. Castelli, F. Fenaille, A. Prignon, F. Alzaid, C. Combes, A. Delvaux, Y. Adimy, M. Cohen-Solal, P. Richette, T. Bardin, J.-P. Riveline, N. Venteclef, F. Lioté, L. Campillo-Gimenez, H.-K. Ea, *Ann. Rheum. Dis.* **2020**, *79*, 1506.
[36] C. A. Poland, R. Duffin, I. Kinloch, A. Maynard, W. A. H. Wallace, A. Seaton, V. Stone, S. Brown, W. Macnee, K. Donaldson, *Nat. Nanotechnol.* **2008**, *3*, 423.
[37] J. Ma, R. Liu, X. Wang, Q. Liu, Y. Chen, R. P. Valle, Y.i Y. Zuo, T. Xia, S. Liu, *ACS Nano* **2015**, *9*, 10498.
[38] S. Park, L. E. Lee, H. Kim, J. E. Kim, S. J. Lee, S. Yoon, S. Shin, H. Kang, Y. Park, J. J. Song, S. Lee, *Scientific Rep.* **2021**, *11*, 10019.
[39] D. J. Allen, G. Milosovich, A. M. Mattocks, *Arthritis Rheum.* **1965**, *8*, 1123.
[40] A. Chhana, G. Lee, N. Dalbeth, *BMC Musculoskelet Disord* **2015**, *16*, 296.
[41] L.-G. M. Sansano, E. Rodríguez-Alvear, C. Calabuig-Sais, I. Martínez-Sanchís, A. Pascual, E. Andrés, *Arthritis Rheumatol.* **2023**.
[42] M. Liu, W. Liu, X. Liu, Y. Wang, Z. Wei, *Nano Today* **2021**, *2*, 37.
[43] Q. Du, D. Ge, V. Mirshafiee, C. Chen, M. Li, C. Xue, X. Ma, B. Sun, *Nanoscale* **2019**, *11*, 12965.
[44] H. Yin, L. Fang, L. Wang, Y. Xia, J. Tian, L. Ma, J. Zhang, N. Li, W. Li, S. Yao, L. Zhang, *Front Immunol* **2022**, *13*, 874459.
[45] C. Schorn, C. Janko, V. Krenn, Y. Zhao, L. E. Munoz, G. Schett, M. Herrmann, *Front Immunol* **2012**, *3*, 376.
[46] J. Desai, S. V. Kumar, S. R. Mulay, L. Konrad, S. Romoli, C. Schauer, M. Herrmann, R. Bilyy, S. Müller, B. Popper, D. Nakazawa, M. Weidenbusch, D. Thomasova, S. Krautwald, A. Linkermann, H.-J. Anders, *Eur. J. Immunol.* **2016**, *46*, 223.
[47] I. Mitroulis, K. Kambas, A. Chrysanthopoulou, P. Skendros, E. Apostolidou, I. Kourtzelis, G. I. Drosos, D. T. Boumpas, K. Ritis, *PLoS One* **2011**, *6*, 29318.
[48] A. K. Meher, M. Spinosa, J. P. Davis, N. Pope, V. E. Laubach, G. Su, V. Serbulea, N. Leitinger, G. Ailawadi, G. R. Upchurch, *Arterioscler Thromb Vasc Biol* **2018**, *38*, 843.
[49] B.o Yan, P. Han, L. Pan, W. Lu, J. Xiong, M. Zhang, W. Zhang, L.i Li, Z. Wen, *J. Immunol.* **2014**, *192*, 5998.
[50] A. Singh, K. A. Zarember, D. B. Kuhns, J. I. Gallin, *J. Immunol.* **2009**, *182*, 6410.
[51] B. Sun, X. Wang, Z. Ji, M. Wang, Y.u-P. Liao, C. H. Chang, R. Li, H. Zhang, A. E. Nel, T. Xia, *Small* **2015**, *11*, 2087.
[52] L. Chen, Y. Zhao, D. Lai, P. Zhang, Y. Yang, Y. Li, K. Fei, G. Jiang, J. Fan, *Cell Death Dis.* **2018**, *9*, 576.
[53] Y. Cui, Y. Yang, W. Tao, W. Peng, D. Luo, N. Zhao, S. Li, K. Qian, F. Liu, *J Inflamm Res* **2023**, *16*, 861.
[54] H. Li, Y.i Li, C. Song, Y. Hu, M. Dai, B. Liu, P. Pan, *J Inflamm Res* **2021**, *14*, 4839.
[55] C. Liu, Y. Zhou, Q. Tu, L. Yao, J. Li, Z. Yang, *Front Immunol* **2023**, *14*, 1146612.
[56] C. M. S. Silva, C. W. S. Wanderley, F. P. Veras, F. Sonego, D. C. Nascimento, A. V. Gonçalves, T. V. Martins, D. F. Cólon, V. F. Borges, V. S. Brauer, L. E. A. Damasceno, K. P. Silva, J. E. Toller-Kawahisa, S. S. Batah, A. L. J. Souza, V. S. Monteiro, A. E. R. Oliveira, P. B. Donate, D. Zoppi, M. C. Borges, F. Almeida, H. I. Nakaya, A. T. Fabro, T. M. Cunha, J. C. Alves-Filho, D. S. Zamboni, F. Q. Cunha, *Blood* **2021**, *138*, 2702.
[57] S.-M. Ye, M.-Z.e Zhou, W.-J. Jiang, C.-X. Liu, Z.-W. Zhou, M.-J. Sun, Q.-H. Hu, *Mol. Pharmaceutics* **2021**, *18*, 667.
[58] B. Tastan, B. I. Arioz, K. U. Tufekci, E. Tarakcioglu, C. P. Gonul, K. Genc, S. Genc, *Front Immunol* **2021**, *12*, 737065.
[59] B. A. McKenzie, M. K. Mamik, L. B. Saito, R. Boghozian, M. C. Monaco, E. O. Major, J. Q. Lu, W. G. Branton, C. Power, *Proc. Natl. Acad. Sci. USA* **2018**, *115*, E6065.
[60] L. Kang, J. Dai, Y. Wang, P. Shi, Y. Zou, J. Pei, Y. Tian, J.i Zhang, V. C. Buranasudja, J. Chen, H. Cai, X. Gao, Z. Lin, *PLoS Genet.* **2022**, *18*, 1010515.